

Supporting Information for:

Kinetic Control of Anion Stoichiometry in

Hexagonal BaTiO₃

*Keisuke Kageyama*¹, *Yang Yang*¹, *Toki Kageyama*¹, *Kantaro Murayama*¹, *Kazuki Shitara*²,
Takashi Saito^{3, 4, 5}, *Hiroki Ubukata*¹, *Cédric Tassel*¹, *Akihide Kuwabara*² and *Hiroshi*
Kageyama^{1,*}

¹ Department of Energy and Hydrocarbon Chemistry, Graduate School of Engineering, Kyoto University, Nishikyo-ku, Kyoto 615-8510, Japan

² Nanostructures Research Laboratory, Japan Fine Ceramics Center, 2-4-1 Mustuno, Atsuta-ku, Nagoya 456-8587, Japan

³ Institute of Materials Structure Science, High Energy Accelerator Research Organization (KEK), Tokai, Ibaraki 319-1106, Japan

⁴ Materials and Life Science Division, J-PARC Center, Tokai, Ibaraki 319-1195, Japan

⁵ SOKENDAI (School of High Energy Accelerator Science, the Graduate University for Advanced Studies), Tokai, Ibaraki 319-1195, Japan

* Correspondence: kage@scl.kyoto-u.ac.jp (H.K.)

Table of contents

Figure S1. Results of (a) thermogravimetric analysis which was performed in oxygen flow at a rate of 300 ml/min, and (b) quadruple mass spectrometry of H₂, the sample was heated in flowing O₂ at a rate of 300 ml/min. The specimen of BTOH-L2 prepared by hydride reduction of BTO-L with CaH₂ at 520 °C for 120 hours was selected in the experiment.

Figure S2. The relationship between lattice parameters (a) *c*, (b) *a* and reaction time for the h-BaTiO_{3-x}H_x reduced by H₂ at 1450 °C for 1 hour and hydrogenated with CaH₂ at 520 °C.

Figure S3. SEM images of 6H BaTiO_{3-x}. (a) Specimen prepared by H₂ reduction at 1450 °C for 1 hour (BTO-L). (b) Specimen prepared by Mg reduction twice at 1000 °C for 10 hours (BTO-S).

Figure S4. Variation of hydrogen content in h-BaTiO_{3-x}H_x as a function of hydrogenation temperature by CaH₂ reduction. The hydrogen content is assumed to be equivalent to oxygen deficiency in SXRD analysis, whereas it was directly refined for the ND data (Table S3).

Figure S5. The (a) 1st, (b) 2nd, and (c) 5th most stable structures in 6H-type system for Ba₆Ti₆O₁₆H₂ obtained by the DFT calculations. Gray, light blue, red and blue balls represent Ba, Ti, O, H atoms, respectively.

Figure S6. Relationship between predicted values from LASSO regression and calculated values for Ba₆Ti₆O₁₆H₂.

Figure S7. Obtained coefficients from LASSO regression. In h-BaTiO_{3-x}H_x, hydride anions are more likely to occupy the face-sharing site and have weaker *cis/trans* preference.

Table S1. Sample lists. (a) BaTiO₃ (BT03, Sakai) was reduced in H₂ atmosphere and hydrided by CaH₂. (b), (c), (d) and (e) BaTiO₃ (BT01, Sakai) were prepared by Mg reduction method and hydrided by CaH₂.

Table S2. Number of symmetrically independent O/H configurations of a hexagonal unit cell with the composition of $\text{Ba}_6\text{Ti}_6\text{O}_{18-n}\text{H}_n$ ($n = 1 \sim 6$).

Table S3. Crystallographic parameters of h-BaTiO_{3-x} with varied oxygen deficiency prepared by Mg reduction.

Table S4. Crystallographic data analyzed by the Rietveld analysis against SXRD and the NPD patterns of h-BaTiO_{3-x}H_x prepared by Mg reduction in different conditions. In SXRD analysis, oxygen deficiency is assumed to be filled by H⁻ anion. Ti³⁺/Ti⁴⁺ ratios were estimated with the formula of $\text{BaTi}^{3+}_x\text{Ti}^{4+}_{1-x}\text{O}_{3-x}\text{H}_x$.

Table S5. List of descriptors of structural parameters.

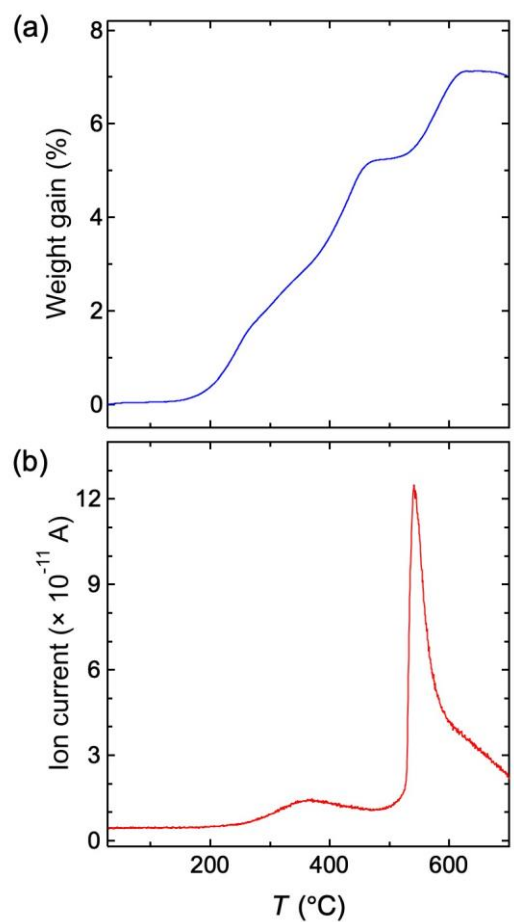


Figure S1. Results of (a) thermogravimetric analysis which was performed in oxygen flow at a rate of 300 ml/min, and (b) quadrupole mass spectrometry of H_2 , the sample was heated in flowing O_2 at a rate of 300 ml/min. The specimen of BTOH-L2 prepared by hydride reduction of BTO-L with CaH_2 at 520 °C for 120 hours was selected in the experiment.

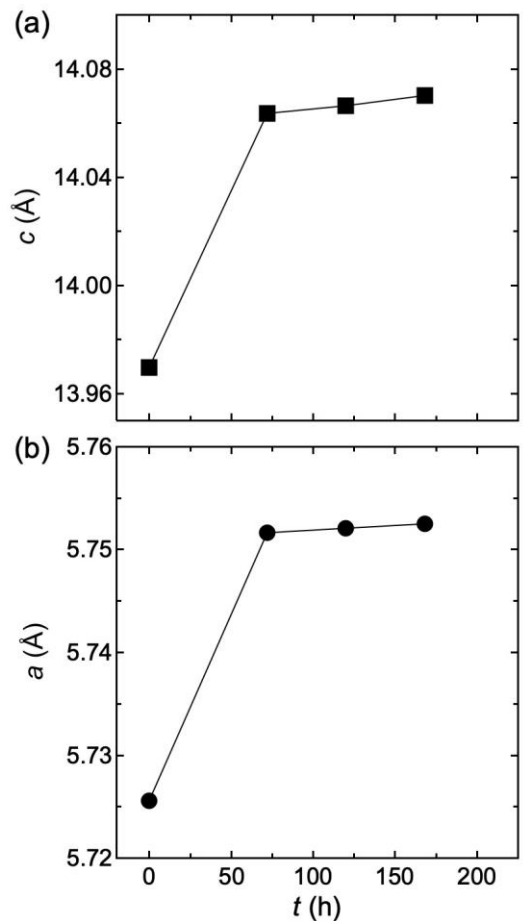


Figure S2. The relationship between lattice parameters (a) c , (b) a and reaction time for the $\text{h-BaTiO}_{3-x}\text{H}_x$ reduced by H_2 at 1450°C for 1 hour and hydrogenated with CaH_2 at 520°C .

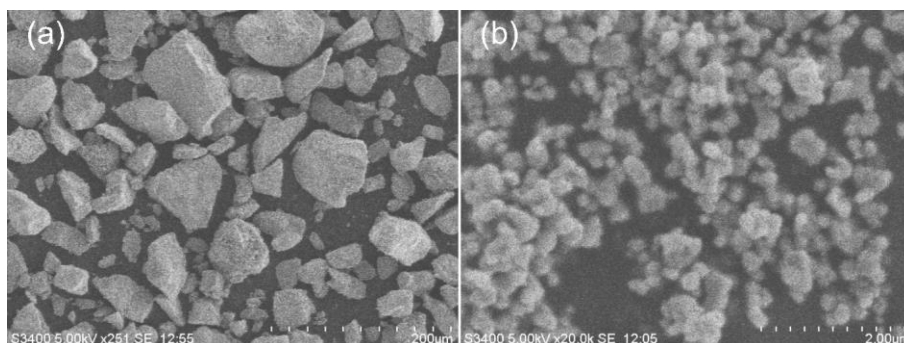


Figure S3. SEM images of 6H BaTiO_{3-x} . (a) Specimen prepared by H_2 reduction at 1450°C for 1 hour (BTO-L). (b) Specimen prepared by Mg reduction twice at 1000°C for 10 hours (BTO-S).

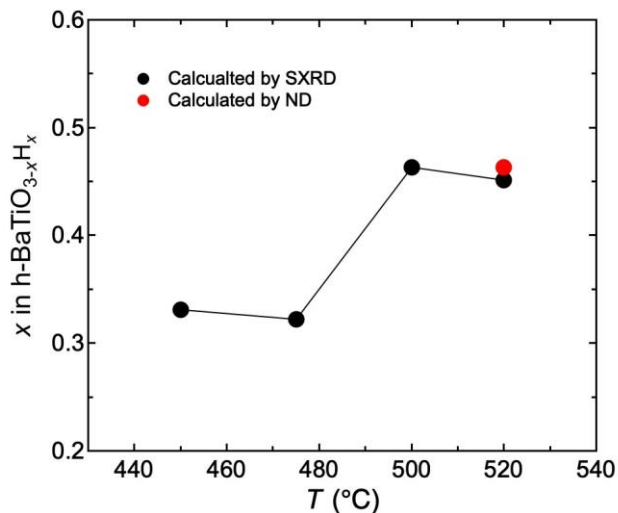


Figure S4. Variation of hydrogen content in $\text{h-BaTiO}_{3-x}\text{H}_x$ as a function of hydrogenation temperature by CaH_2 reduction. The hydrogen content is assumed to be equivalent to oxygen deficiency in SXR analysis, whereas it was directly refined for the NPD data (Table S3).

Regression analysis of energy calculations

Formation energies for each structure parameters were analyzed with linear regression method as to the hexagonal $\text{BaTiO}_{3-x}\text{H}_x$ structures in order to analyze the most important structural parameter for the formation energies. The 1496 independent configurations shown in Table S2 were constructed and have been calculated. Then, the formation energies were standardized for each composition in order to remove too large influence of hydrogen amounts. The structural parameters used in regression analysis are shown in Table S5. The database was standardized before the analysis. Linear regression analysis was performed using least absolute shrinkage and selection operator (LASSO) [35], which is one of the least squared methods with the regularization term. The magnitude of the absolute value of the coefficients corresponds to the importance of the parameters, and the sign of the coefficients corresponds to positive or negative correlation between the formation energies and the parameters.

Figure S6 shows the relationship between predicted values from LASSO regression and calculated values. The obtained coefficients with the regression were presented in Figure S7. The coefficients of N_{face} and N_{trans} have large negative value, which implies that H^- anion energetically prefers the face-sharing site and *trans*-coordination. These results support the site selectivity of H^- in the hexagonal $\text{BaTiO}_{3-x}\text{H}_x$ structures discussed in the text.

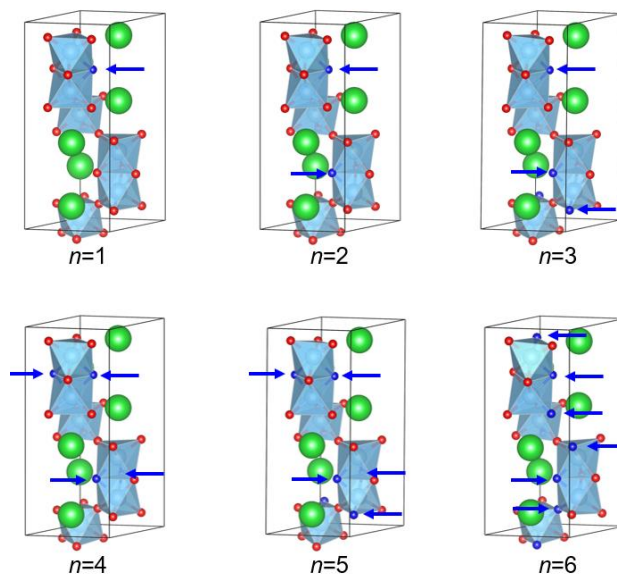


Figure S5. Most stable structures in 6H-type system for $\text{Ba}_6\text{Ti}_6\text{O}_{18-n}\text{H}_n$ for $n = 1 \sim 6$. Green, light blue, red, and blue balls represent Ba, Ti, O, and H atoms, respectively.

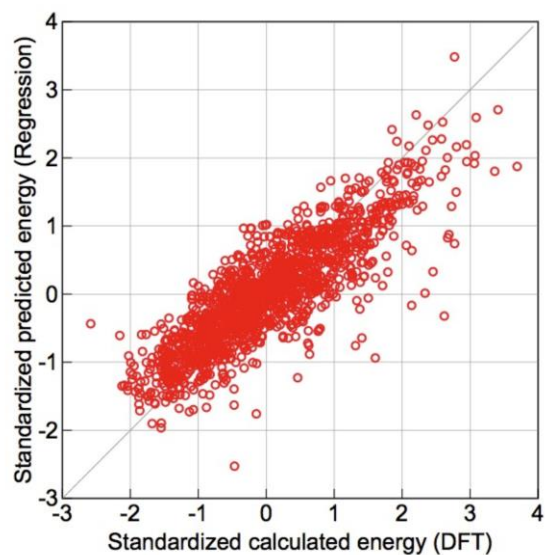


Figure S6. Relationship between predicted energies from LASSO regression and DFT calculations for $\text{Ba}_6\text{Ti}_6\text{O}_{18-n}\text{H}_n$.

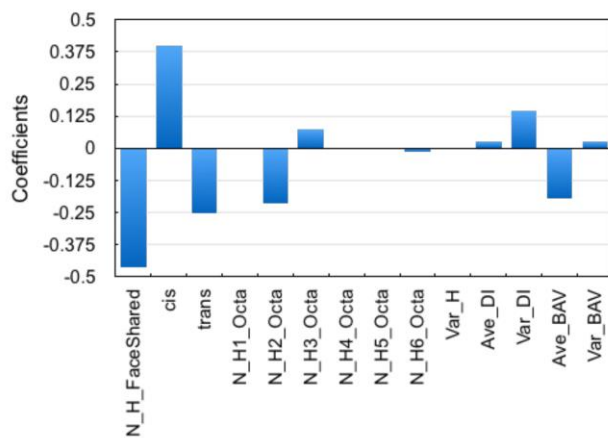


Figure S7. Obtained coefficients from LASSO regression. In $\text{h-BaTiO}_{3-x}\text{H}_x$, hydride anions are more likely to occupy the face-sharing site and have weaker *cis/trans* preference.

Table S1. Sample lists. (a) BaTiO₃ (BT03, Sakai) was reduced in H₂ atmosphere and hydrided by CaH₂. (b), (c), (d) and (e) BaTiO₃ (BT01, Sakai) were prepared by Mg reduction method and hydrided by CaH₂.

(a)	BaTiO _{3-x}	⇒	BaTiO _{3-x} H _x		
	H ₂ reduction		CaH ₂ Hydrogenation		
Specimen	L-1		L-1-1	L-1-2	L-1-3
Condition	1450 °C/1 h		520 °C/72 h	520 °C/120 h	520 °C/168 h
(b)	BaTiO _{3-x}	⇒	BaTiO _{3-x} H _x		
	Mg reduction		CaH ₂ Hydrogenation		
Specimen	S-1		S-1-1	S-1-2	S-1-3
Condition	1) 950 °C/10 h 2) 1000 °C/10 h		450 °C/120 h	475 °C/120 h	500 °C/120 h
(c)	BaTiO _{3-x}	⇒	BaTiO _{3-x} H _x		
	Mg reduction		CaH ₂ Hydrogenation		
Specimen	S-2		S-2-1	S-2-2	
Condition	1) 1000 °C/10 h 2) 1000 °C/10 h		475 °C/120 h	520 °C/120 h	
(d)	BaTiO _{3-x}	⇒	BaTiO _{3-x} H _x		
	Mg reduction		CaH ₂ Hydrogenation		
Specimen	S-3		S-3-1		
Condition	1) 1025 °C/10 h 2) 950 °C/10 h		475 °C/120 h		
(e)	BaTiO _{3-x}	⇒	BaTiO _{3-x} H _x		
	Mg reduction		CaH ₂ Hydrogenation		
Specimen	S-4		S-4-1		
Condition	1) 1025 °C/10 h 2) 1000 °C/10 h		475 °C/120 h		

Table S2. Number of symmetrically independent O/H configurations of a hexagonal unit cell with the composition of $\text{Ba}_6\text{Ti}_6\text{O}_{18-n}\text{H}_n$ ($n = 1 \sim 6$).

n in $\text{Ba}_6\text{Ti}_6\text{O}_{18-n}\text{H}_n$	Number of symmetrically independent O/H configurations
1	2
2	14
3	46
4	164
5	400
6	870
Total	1496

Table S3-1. Crystallographic parameters for the hexagonal BaTiO_{2.72} (S-1) from SXRDR refinement^a

atom	site	g^b	x	y	z	$B_{\text{iso}} (\text{\AA}^2)$
Ba1	2 <i>b</i>	1	0	0	0.25	0.45(1)
Ba2	4 <i>f</i>	1	0.333333	0.666667	0.09291(5)	0.57(1)
Ti1	2 <i>a</i>	1	0	0	0	0.37(3)
Ti2	4 <i>f</i>	1	0.333333	0.666667	0.8503(1)	0.53(3)
O1	6 <i>h</i>	0.72(1)	0.5260(6)	0.052	0.25	0.6(1)
O2	12 <i>k</i>	1	0.8294(4)	0.6588	0.0835(2)	0.43(5)

^aSpace group: *P6₃/mmc*; $Z = 6$; $a = 5.7476(1) \text{\AA}$, and $c = 14.0608(1) \text{\AA}$; $R_p = 6.16\%$, $R_{wp} = 8.17\%$, $R_B = 5.69\%$, $R_F = 11.50\%$, and $\text{GOF} = 1.42$ for SXRDR. g^b represents the occupancy factor of each site.

Table S3-2. Crystallographic parameters for the hexagonal BaTiO_{2.72} (S-2) from SXRDR refinement^a

atom	site	g^b	x	y	z	$B_{\text{iso}} (\text{\AA}^2)$
Ba1	2 <i>b</i>	1	0	0	0.25	0.503(7)
Ba2	4 <i>f</i>	1	0.333333	0.666667	0.08857(5)	0.589(5)
Ti1	2 <i>a</i>	1	0	0	0	0.52(2)
Ti2	4 <i>f</i>	1	0.333333	0.666667	0.8498(1)	0.48(2)
O1	6 <i>h</i>	0.72(1)	0.527(2)	0.054	0.25	1.20(1)
O2	12 <i>k</i>	1	0.8299(9)	0.6599	0.0842(2)	0.47(4)

^aSpace group: *P6₃/mmc*; $Z = 6$; $a = 5.7526(1) \text{\AA}$, and $c = 14.0852(1) \text{\AA}$; $R_p = 5.49\%$, $R_{wp} = 8.53\%$, $R_B = 3.47\%$, $R_F = 3.17\%$, and $\text{GOF} = 5.50$ for SXRDR. g^b represents the occupancy factor of each site.

Table S3-3. Crystallographic parameters for the hexagonal BaTiO_{2.76} (S-3) from SXRD refinement^a

atom	site	g^b	x	y	z	$B_{\text{iso}} (\text{Å}^2)$
Ba1	2 <i>b</i>	1	0	0	0.25	0.40(1)
Ba2	4 <i>f</i>	1	0.333333	0.666667	0.09360(5)	0.46(1)
Ti1	2 <i>a</i>	1	0	0	0	0.21(3)
Ti2	4 <i>f</i>	1	0.333333	0.666667	0.8497(1)	0.57(3)
O1	6 <i>h</i>	0.76(1)	0.5242(5)	0.0485	0.25	0.4(1)
O2	12 <i>k</i>	1	0.8308(4)	0.6615	0.0826(3)	0.33(4)

^aSpace group: $P6_3/mmc$; $Z = 6$; $a = 5.7426(1) \text{ Å}$, and $c = 14.0337(1) \text{ Å}$; $R_p = 6.24\%$, $R_{wp} = 9.16\%$, $R_B = 5.42\%$, $R_F = 3.12\%$, and $\text{GOF} = 2.89$ for SXRD. g^b represents the occupancy factor of each site.

Table S3-4. Crystallographic parameters for the hexagonal BaTiO_{2.74} (S-4) from SXRD refinement^a

atom	site	g^b	x	y	z	$B_{\text{iso}} (\text{Å}^2)$
Ba1	2 <i>b</i>	1	0	0	0.25	0.494(6)
Ba2	4 <i>f</i>	1	0.333333	0.666667	0.09297(3)	0.602(4)
Ti1	2 <i>a</i>	1	0	0	0	0.52(2)
Ti2	4 <i>f</i>	1	0.333333	0.666667	0.84990(8)	0.52(2)
O1	6 <i>h</i>	0.74(1)	0.5256(12)	0.0513	0.25	0.83(9)
O2	12 <i>k</i>	1	0.8308(7)	0.6615	0.0834(2)	0.52(4)

^aSpace group: $P6_3/mmc$; $Z = 6$; $a = 5.7476(1) \text{ Å}$, and $c = 14.0585(1) \text{ Å}$; $R_p = 5.00\%$, $R_{wp} = 7.85\%$, $R_B = 3.00\%$, $R_F = 3.21\%$, and $\text{GOF} = 5.12$ for SXRD. g^b represents the occupancy factor of each site.

Table S3-5. Summary of the lattice parameters for the hexagonal BaTiO_{3-x} from SXRD refinement^a

Sample	x	a (Å)	c (Å)	V (Å ³)
S-1	0.28(1)	5.7476(1)	14.0608(1)	402.268
S-2	0.28(1)	5.7526(1)	14.0852(1)	403.664
S-3	0.24(1)	5.7426(1)	14.0337(1)	400.786
S-4	0.26(1)	5.7476(1)	14.0585(1)	402.206

^aSpace group: $P6_3/mmc$; $Z = 6$.

Table S4-1. Crystallographic parameters for the hexagonal BaTiO_{2.67}H_{0.33} (S-1-1) from SXRD refinement^a. H⁻ content is estimated from the occupancy (*g*) of oxygen assuming oxygen deficits are filled with H⁻ anions. Ti³⁺/Ti⁴⁺ ratios were estimated with the formula of BaTi³⁺_{*x*}Ti⁴⁺_{1-*x*}O_{3-*x*}H_{*x*}.

atom	site	<i>g</i> ^{<i>b</i>}	<i>x</i>	<i>y</i>	<i>z</i>	<i>B</i> _{iso} (Å ²)
Ba1	2 <i>b</i>	1	0	0	0.25	0.569(8)
Ba2	4 <i>f</i>	1	0.333333	0.666667	0.09134(5)	0.733(6)
Ti1	2 <i>a</i>	1	0	0	0	0.52(2)
Ti2	4 <i>f</i>	1	0.333333	0.666667	0.8500(1)	0.57(2)
O1	6 <i>h</i>	0.67(1)	0.528(2)	0.0566	0.25	1.20(2)
O2	12 <i>k</i>	1	0.83(1)	0.6615	0.0841(2)	0.62(5)

^aSpace group: *P*6₃/*m**m**c*; *Z* = 6; *a* = 5.7567(1) Å, and *c* = 14.0905(1) Å; *R*_p = 6.49%, *R*_{wp} = 9.21%, *R*_B = 4.60%, *R*_F = 10.67%, and GOF = 2.74 for SXRD. Ti³⁺/Ti⁴⁺ = 0.33/0.67. *g*^{*b*} represents the occupancy factor of each site.

Table S4-2. Crystallographic parameters for the hexagonal BaTiO_{2.68}H_{0.32} (S-1-2) from SXRD refinement^a. H⁻ content is estimated from the occupancy (*g*) of oxygen assuming oxygen deficits are filled with H⁻ anions. Ti³⁺/Ti⁴⁺ ratios were estimated with the formula of BaTi³⁺_{*x*}Ti⁴⁺_{1-*x*}O_{3-*x*}H_{*x*}.

atom	site	<i>g</i> ^{<i>b</i>}	<i>x</i>	<i>y</i>	<i>z</i>	<i>B</i> _{iso} (Å ²)
Ba1	2 <i>b</i>	1	0	0	0.25	0.560(9)
Ba2	4 <i>f</i>	1	0.333333	0.666667	0.09054(6)	0.719(7)
Ti1	2 <i>a</i>	1	0	0	0	0.36(3)
Ti2	4 <i>f</i>	1	0.333333	0.666667	0.8499(2)	0.60(4)
O1	6 <i>h</i>	0.68(1)	0.526(2)	0.0511	0.25	0.92(5)
O2	12 <i>k</i>	1	0.8274(5)	0.6548	0.0843(2)	0.47(6)

^aSpace group: *P*6₃/*m**m**c*; *Z* = 6; *a* = 5.7589(1) Å, and *c* = 14.0892(1) Å; *R*_p = 7.51%, *R*_{wp} = 10.54%, *R*_B = 5.19%, *R*_F = 10.23%, and GOF = 3.76 for SXRD. Ti³⁺/Ti⁴⁺ = 0.32/0.68. *g*^{*b*} represents the occupancy factor of each site.

Table S4-3. Crystallographic parameters for the hexagonal BaTiO_{2.54}H_{0.46} (S-1-3) from SXRD refinement^a. H⁻ content is estimated from the occupancy (*g*) of oxygen assuming oxygen deficits are filled with H⁻ anions. Ti³⁺/Ti⁴⁺ ratios were estimated with the formula of BaTi³⁺_{*x*}Ti⁴⁺_{1-*x*}O_{3-*x*}H_{*x*}.

atom	site	<i>g</i> ^{<i>b</i>}	<i>x</i>	<i>y</i>	<i>z</i>	<i>B</i> _{iso} (Å ²)
Ba1	2 <i>b</i>	1	0	0	0.25	0.603(13)
Ba2	4 <i>f</i>	1	0.333333	0.666667	0.08970(7)	0.732(9)
Ti1	2 <i>a</i>	1	0	0	0	0.51(4)
Ti2	4 <i>f</i>	1	0.333333	0.666667	0.8493(2)	0.57(4)
O1	6 <i>h</i>	0.54(1)	0.5322(2)	0.0643	0.25	0.46(6)
O2	12 <i>k</i>	1	0.8294(6)	0.6608	0.0802(3)	0.46(6)

^aSpace group: *P63/mmc*; *Z* = 6; *a* = 5.7604(1) Å, and *c* = 14.0830(1) Å; *R*_p = 7.32%, *R*_{wp} = 9.88%, *R*_B = 8.77%, *R*_F = 13.81%, and GOF = 5.76 for SXRD. Ti³⁺/Ti⁴⁺ = 0.46/0.54. *g*^{*b*} represents the occupancy factor of each site.

Table S4-4. Crystallographic parameters for the hexagonal BaTiO_{2.66}H_{0.34} (S-2-1) from SXRD refinement^a. H⁻ content is estimated from the occupancy (*g*) of oxygen assuming oxygen deficits are filled with H⁻ anions. Ti³⁺/Ti⁴⁺ ratios were estimated with the formula of BaTi³⁺_{*x*}Ti⁴⁺_{1-*x*}O_{3-*x*}H_{*x*}.

atom	site	<i>g</i> ^{<i>b</i>}	<i>x</i>	<i>y</i>	<i>z</i>	<i>B</i> _{iso} (Å ²)
Ba1	2 <i>b</i>	1	0	0	0.25	0.452(7)
Ba2	4 <i>f</i>	1	0.333333	0.666667	0.09118(3)	0.579(5)
Ti1	2 <i>a</i>	1	0	0	0	0.36(2)
Ti2	4 <i>f</i>	1	0.333333	0.666667	0.85019(8)	0.47(2)
O1	6 <i>h</i>	0.66(1)	0.5259(5)	0.05176687	0.25	1.4(1)
O2	12 <i>k</i>	1	0.8295(3)	0.659	0.0845(1)	0.44(3)

^aSpace group: *P63/mmc*; *Z* = 6; *a* = 5.7572(2) Å, and *c* = 14.0876(1) Å; *R*_p = 4.92%, *R*_{wp} = 6.86%, *R*_B = 2.70%, *R*_F = 2.30%, and GOF = 4.22 for SXRD. Ti³⁺/Ti⁴⁺ = 0.34/0.66. *g*^{*b*} represents the occupancy factor of each site.

Table S4-5. Crystallographic parameters for the hexagonal BaTiO_{2.55}H_{0.45} (S-2-2) from SXR (upper) and those of h-BaTiO_{2.4}H_{0.6} (S-2-2) from Time-of-Flight NPD (lower) refinement^a. H⁻ content is estimated from the occupancy (*g*) of oxygen assuming oxygen deficits are filled with H⁻ anions. Ti³⁺/Ti⁴⁺ ratios were estimated with the formula of BaTi³⁺_{*x*}Ti⁴⁺_{1-*x*}O_{3-*x*}H_{*x*}.

atom	site	<i>g</i> ^{<i>b</i>}	<i>x</i>	<i>y</i>	<i>z</i>	<i>B</i> _{iso} (Å ²)
Ba1	2 <i>b</i>	1	0	0	0.25	0.574(19)
						0.258(4)
Ba2	4 <i>f</i>	1	0.333333	0.666667	0.08857(9)	0.568(10)
						0.0948(2)
Ti1	2 <i>a</i>	1	0	0	0	0.53(5)
						0.48(5)
Ti2	4 <i>f</i>	1	0.333333	0.666667	0.8485(2)	0.49(4)
						0.8644(3)
O1	6 <i>h</i>	0.55(1)	0.533(1)	0.0652	0.25	0.89(3)
		0.54(1)	0.5312(5)	0.0625	0.25	1.10(2)
H1	6 <i>h</i>	0.46(1)	0.5312(5)	0.0625	0.25	1.10(2)
O2	12 <i>k</i>	1	0.8331(7)	0.6662	0.0865(4)	0.66(9)
		1	0.8284(2)	0.6573	0.08920(1)	0.42(2)
H2	12 <i>k</i>					

^aSpace group: *P63/mmc*; *Z* = 6; *a* = 5.7664(1) Å, and *c* = 14.0713(1) Å for SXR and *a* = 5.76499(6) Å and *c* = 14.0792(3) Å for NPD. *R*_p = 8.93%, *R*_{wp} = 12.85%, *R*_B = 10.94%, *R*_F = 9.77%, and GOF = 2.23 for SXR and *R*_p = 1.57%, *R*_{wp} = 2.07%, *R*_B = 16.97%, *R*_F = 15.15%, and GOF = 3.96 for NPD. Ti³⁺/Ti⁴⁺ = 0.45/0.55 for SXR and Ti³⁺/Ti⁴⁺ = 0.46/0.54 for ND. *g*^{*b*} represents the occupancy factor of each site.

Table S4-6. Crystallographic parameters for the hexagonal BaTiO_{2.69}H_{0.31} (S-3-1) from SXRDR refinement^a. H⁻ content is estimated from the occupancy (*g*) of oxygen assuming oxygen deficits are filled with H⁻ anions. Ti³⁺/Ti⁴⁺ ratios were estimated with the formula of BaTi³⁺_{*x*}Ti⁴⁺_{1-*x*}O_{3-*x*}H_{*x*}.

atom	site	<i>g</i> ^{<i>b</i>}	<i>x</i>	<i>y</i>	<i>z</i>	<i>B</i> _{iso} (Å ²)
Ba1	2 <i>b</i>	1	0	0	0.25	0.46(3)
Ba2	4 <i>f</i>	1	0.333333	0.666667	0.09177(5)	0.48(3)
Ti1	2 <i>a</i>	1	0	0	0	0.46(3)
Ti2	4 <i>f</i>	1	0.333333	0.666667	0.8504(1)	0.49(3)
O1	6 <i>h</i>	0.69(1)	0.5239(6)	0.048	0.25	0.9(1)
O2	12 <i>k</i>	1	0.8297(4)	0.6595	0.0843(2)	0.52(4)

^aSpace group: *P63/mmc*; *Z* = 6; *a* = 5.7540(1) Å, and *c* = 14.0826(1) Å; *R*_p = 5.26%, *R*_{wp} = 7.65%, *R*_B = 3.80%, *R*_F = 2.30%, and GOF = 6.01 for SXRDR. Ti³⁺/Ti⁴⁺ = 0.31/0.69. *g*^{*b*} represents the occupancy factor of each site.

Table S4-7. Crystallographic parameters for the hexagonal BaTiO_{2.73}H_{0.27} (S-4-1) from SXRDR refinement^a. H⁻ content is estimated from the occupancy (*g*) of oxygen assuming oxygen deficits are filled with H⁻ anions. Ti³⁺/Ti⁴⁺ ratios were estimated with the formula of BaTi³⁺_{*x*}Ti⁴⁺_{1-*x*}O_{3-*x*}H_{*x*}.

atom	site	<i>g</i> ^{<i>b</i>}	<i>x</i>	<i>y</i>	<i>z</i>	<i>B</i> _{iso} (Å ²)
Ba1	2 <i>b</i>	1	0	0	0.25	0.51(2)
Ba2	4 <i>f</i>	1	0.333333	0.666667	0.09261(6)	0.59(1)
Ti1	2 <i>a</i>	1	0	0	0	0.40(3)
Ti2	4 <i>f</i>	1	0.333333	0.666667	0.8510(1)	0.54(4)
O1	6 <i>h</i>	0.73(1)	0.5271(8)	0.05413413	0.25	1.5(2)
O2	12 <i>k</i>	1	0.8308(5)	0.6615	0.0835(3)	0.61(6)

^aSpace group: *P63/mmc*; *Z* = 6; *a* = 5.7481(1) Å, and *c* = 14.0671(1) Å; *R*_p = 6.75%, *R*_{wp} = 10.74%, *R*_B = 6.34%, *R*_F = 5.50%, and GOF = 9.84 for SXRDR. Ti³⁺/Ti⁴⁺ = 0.27/0.73. *g*^{*b*} represents the occupancy factor of each site.

Table S4-8. Summary of lattice parameters and $\text{Ti}^{3+}/\text{Ti}^{4+}$ ratio for the hexagonal $\text{BaTiO}_{3-x}\text{H}_x$ from SXRD refinement^a and NPD refinement^a (S-2-2, lower). H^- content is estimated from the occupancy (*g*) of oxygen assuming oxygen deficits are filled with H^- anions. $\text{Ti}^{3+}/\text{Ti}^{4+}$ ratios were estimated with the formula of $\text{BaTi}_x^{3+}\text{Ti}_{1-x}^{4+}\text{O}_{3-x}\text{H}_x$.

Sample	<i>x</i>	<i>a</i> (Å)	<i>c</i> (Å)	<i>V</i> (Å ³)	$\text{Ti}^{3+}/\text{Ti}^{4+}$
S-1-1	0.33(1)	5.7567(1)	14.0905(1)	404.392	0.33/0.67
S-1-2	0.32(1)	5.7589(1)	14.0892(1)	404.661	0.32/0.68
S-1-3	0.46(1)	5.7604(1)	14.0830(1)	404.699	0.46/0.54
S-2-1	0.34(1)	5.7572(2)	4.0876(1)	404.381	0.34/0.66
S-2-2	0.45(1)	5.7664(1)	14.0713(1)	405.198	0.45/0.55
	0.46(1)	5.76499(6)	14.0792(3)	405.233	0.46/0.54
S-3-1	0.31(1)	5.7540(1)	14.0826(1)	403.791	0.31/0.69
S-4-1	0.27(1)	5.7481(1)	14.0671(1)	402.522	0.27/0.73

Table S5. List of descriptors of structural parameters.

Descriptor	Brief description
<i>cis</i>	Number of <i>cis</i> -configurations in the structure
<i>trans</i>	Number of <i>trans</i> -configurations in the structure
N_H_FaceShared	Number of hydrogen atoms at face-shared sites in the structure
N_Hn-Octa ($n = 1 \sim 6$)	Number of octahedra with n hydrogen atoms
Var_H	Variance of hydrogen atoms in octahedra
Av_DI	Average of Baur's distortion index of octahedra
Var_DI	Variance of Baur's distortion index of octahedra
Av_BAV	Average of bond angle variance of octahedra
Var_BAV	Variance of bond angle variance of octahedra